

L. Xiang, F. Pei, and A. Klein, “Joint Optimization of Beamforming and 3D Array Steering for Multi-antenna UAV Communications”, in *IEEE Wireless Communications and Networking Conference (WCNC)*, Dubai, United Arab Emirates, Apr. 2024.

©2024 IEEE. Personal use of this material is permitted. However, permission to reprint/republish this material for advertising or promotional purposes or for creating new collective works for resale or redistribution to servers or lists, or to reuse any copyrighted component of this works must be obtained from the IEEE.

Joint Optimization of Beamforming and 3D Array Steering for Multi-antenna UAV Communications

Lin Xiang, Fengcheng Pei, and Anja Klein

Communications Engineering Lab, Technical University of Darmstadt, Germany

Email: {l.xiang, f.pei, a.klein}@nt.tu-darmstadt.de

Abstract—In this paper, we consider unmanned aerial vehicle (UAV)-aided downlink communication using a *rotatable array of directional antennas* such as half-wavelength dipoles. The antenna array is mounted onboard the UAV using a gimbal and can be flexibly rotated in the three-dimensional (3D) space. As such, the directional gain pattern of dipoles and the array beamforming can be both best exploited to facilitate efficient information transmission to multiple low-priority (or secondary) users while mitigating co-channel interference for another high-priority (or primary) user coexisting with but not served by the UAV. Assuming that the direction of the high-priority user is known, we jointly optimize the electrical beamforming and mechanical steering of the rotatable dipole array for maximizing the weighted sum-rate achievable by the low-priority users while minimizing the interference power radiated in the direction of the high-priority user. The formulated optimization problem is nonconvex and generally intractable. Exploiting its special problem structure, we decompose the problem into several convex and manifold optimization subproblems and further propose a low-complexity iterative algorithm based on proximal block coordinate descent for solution. Our simulation results verify the convergence of the proposed algorithm. Moreover, compared with systems employing non-rotatable and rotatable arrays of isotropic antennas, the rotatable dipole array can flexibly adjust the gain patterns in different azimuth and elevation angles to increase the communication throughput by up to 300% and 77%, respectively.

I. INTRODUCTION

Unmanned aerial vehicles (UAVs) have enabled a plethora of applications in wireless communications [1]. However, UAVs usually suffer from limited size, weight and power (SWAP), and scarce radio resources for communication. Moreover, since the UAVs are elevated and can flexibly move in the air, they may cause strong line-of-sight (LoS) interference to terrestrial/aerial users and base stations (BSs) [2]. Further, when communication secrecy is considered, such LoS channels may unfavorably cause data leakage with a high likelihood [3]. Consequently, how to efficiently, reliably, and securely connecting the growing number of UAVs or exploiting them as aerial BSs/relays within the sixth-generation (6G) cellular networks has been a significant research challenge.

In the existing literature, beamforming using arrays of isotropic antennas [4]–[9] and beam shaping by directional antennas [10]–[13] are two key techniques to tackle the aforementioned challenges. With an onboard antenna array, the UAVs can exploit beamforming or joint optimization of beamforming and trajectory planning to enhance the received signal power while mitigating undesired interference [4]–[8]. Due to the SWAP constraint, however, only a small number of antennas can usually be deployed on a UAV, which limits the spatial degrees of freedom (DoFs) for both signal transmission and interference/leakage mitigation. In [9], the authors considered power-efficient cooperative multiple-input multiple-output (MIMO) transmissions using multiple UAVs, each with

a small antenna array, to increase the spatial DoFs while at the cost of increased complexity for UAV coordination. Note that isotropic antennas are only ideal mathematical models and do not exist in practical systems. Hence, other works [10]–[13] as well the third Generation Partnership Project (3GPP) Release 18 [1] have also considered high-gain directional antennas with a compact form for small UAVs. Exploiting the directional antenna gain pattern, narrowly focused beams are generated to enhance communication while minimizing interference radiated from side-lobes. However, due to its small coverage area, the use of single directional antenna may jeopardize network connectivity of the UAV.

Motivated by the research gaps in [4]–[13], this paper aims to extend the beamforming technique in [4]–[8] to UAVs with arrays of directional antennas such as half-wavelength dipoles, instead of isotropic antennas. The interesting research question here is *how to best exploit the beam shaping by directional antenna elements and the beamforming over the antenna array*. Inspired by radar antennas, rather than fixing the antenna/array orientation [4]–[13], we newly consider three-dimensional (3D) rotation of the dipole array enabled by controlling either the UAV's orientation or a gimbal mounted in the UAV. As such, the proposed rotatable dipole array can adjust both the antenna and array gain patterns to optimize the overall antenna gain pattern, which is the product of the former two patterns according to the antenna theory (i.e., the pattern multiplication principle [14]). Note also that the rotatable dipole array can be particularly beneficial when the UAV employs a small antenna array or flies in a confined space or along a fixed path in normal and emergency communication scenarios.

To maximize the performance benefits, we jointly optimize the electrical beamforming and 3D mechanical steering of the rotatable dipole array for maximizing the weighted sum-rate (WSR) while minimizing the radiated interference power. The resulting optimization problem is much more challenging to solve than those in [4]–[8], particularly due to the 3D rotation of the dipole array. To overcome this obstacle, we decompose the problem into several convex and manifold optimization subproblems, and further propose a low-complexity iterative solution tailored to its problem structure. To the best of our knowledge, neither such rotatable antenna array nor its beamforming/rotation optimization has been considered for (aerial) communication yet. Our contributions are as follows:

- We consider joint electrical beamforming and 3D mechanical steering using a rotatable dipole array deployed at a UAV for advanced aerial communication and interference mitigation in the downlink.
- We formulate a nonconvex optimization problem for maximizing the WSR while minimizing the interference power. We further propose a low-complexity iterative algorithm based on the proximal block coordinate descent (BCD) and manifold optimization to solve the optimization problem.

This work has been funded by the LOEWE initiative (Hesse, Germany) within the emergenCITY center and has been supported by the BMBF project Open6GHub under grant 16KISK014 and by DAAD with funds from the German Federal Ministry of Education and Research (BMBF).

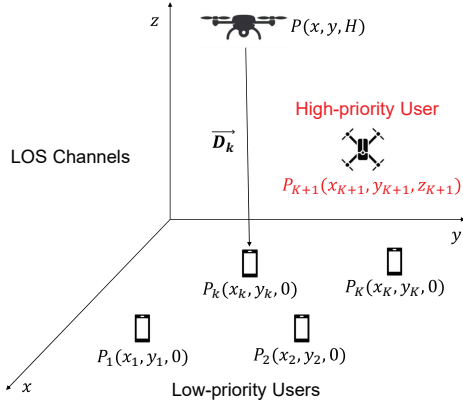


Fig. 1. System model of UAV-aided multiuser communication system.

- Simulation results verify the convergence of the proposed algorithm and show that the rotatable dipole array significantly outperforms the non-rotatable and rotatable arrays with isotropic antenna elements, particularly in scenarios of strong interference, e.g., when users see the same azimuth angle from the UAV.

In the remainder of this paper, we present the system model in Section II. The joint optimization problem of antenna steering and beamforming is formulated and solved via the proposed iterative algorithm in Sections III and IV, respectively. Section V provides the simulation results and finally, Section VI concludes the paper.

Notation: Throughout this paper, matrices and vectors are denoted by boldface capital and lower-case letters, respectively. $\mathbb{C}^{m \times n}$ and $\mathbb{R}^{m \times n}$ denote $m \times n$ complex- and real-valued matrices, respectively. $j = \sqrt{-1}$ is the imaginary unit of a complex number and $\|\cdot\|$ is the l_2 -norm of a vector. \mathbf{A}^T and \mathbf{A}^H are the transpose and complex conjugate transpose of matrix \mathbf{A} , respectively. $\mathbf{a} \circ \mathbf{b}$ is the Hadamard product of vectors \mathbf{a} and \mathbf{b} , and $\text{unit}(\mathbf{a}) = (\frac{a_1}{|a_1|}, \dots, \frac{a_n}{|a_n|})$ forms a vector with unit-norm elements. Finally, $\vec{\mathbf{A}}$ and $\vec{\mathbf{a}}$ denote a displacement vector and its unit direction vector, respectively, which are directional as indicated by $\vec{\cdot}$ and satisfy $\vec{\mathbf{a}}_k = \vec{\mathbf{A}}_k / \|\vec{\mathbf{A}}_k\|$.

II. SYSTEM MODEL

We consider the downlink of a UAV-aided multiuser communication system as shown in Fig. 1. A rotary-wing UAV located at position (x, y, H) aims to transmit data to K low-priority (or secondary) ground/aerial users (though ground/aerial BSs may also be low-priority users, they are ignored here for clarity of presentation). User k is located at position (x_k, y_k, z_k) , $k = 1, \dots, K$. However, a high-priority (or primary) user $K+1$ located at position $(x_{K+1}, y_{K+1}, z_{K+1})$, letting it be e.g. another roaming UAV in the air or a coexisting ground BS, may suffer from strong LoS co-channel interference caused by the UAV. To enhance the signal reception of the low-priority users while mitigating interference to the high-priority user, the UAV employs a rotatable uniform linear array (ULA) with N half-wavelength dipoles for transmit beamforming. Meanwhile, we assume that each user is equipped with a single isotropic receive antenna.

A. 3D Channel Model for Rotatable Dipole Array

As the UAV is elevated, we consider LoS channels between the UAV and all users [9]. The channel between the UAV and

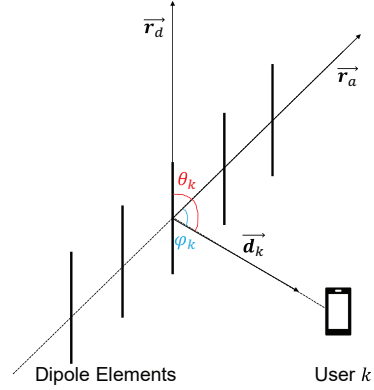


Fig. 2. Relative azimuth and elevation angles of user k .

ground user k is modeled as

$$\mathbf{h}_k = \frac{\sqrt{\beta}}{\|\vec{\mathbf{D}}_k\|} \cdot \mathbf{a}_k, \quad (1)$$

where β is the reference value of path loss at unit distance, $\vec{\mathbf{D}}_k = (x_k - x, y_k - y, z_k - H)^T \in \mathbb{R}^{3 \times 1}$ is the displacement vector from the UAV to user k , and $\mathbf{a}_k \in \mathbb{C}^{N \times 1}$ is the steering vector of the UAV's antenna array. We assume that all users are located in the far field of the UAV. Taking the radiation pattern of the dipoles into account, \mathbf{a}_k is given according to the pattern multiplication principle [14] as

$$\mathbf{a}_k = f_e(\theta_k) \cdot (1, e^{j\frac{2\pi}{\lambda}d \cdot \cos \varphi_k}, \dots, e^{j(N-1)\frac{2\pi}{\lambda}d \cdot \cos \varphi_k})^T, \quad (2)$$

where λ is the carrier frequency and d is the separation of adjacent dipoles in the array. θ_k and φ_k are the angles of user k seen with respect to (w.r.t) the dipole axis and the array axis, respectively, as illustrated in Fig. 2. For convenience, θ_k and φ_k are referred to as the elevation and azimuth angle of user k , respectively, even when the antenna array changes its orientation. Finally, $f_e(\theta_k)$ accounts for the directional dependence of the electric field in each dipole with

$$f_e(\theta_k) = \frac{\cos(\frac{\pi}{2} \cos \theta_k)}{\sin \theta_k} \alpha, \quad (3)$$

where α is a normalization coefficient to ensure that the same total power is radiated in all elevation angles as the ULA with isotropic elements, i.e., $\frac{1}{2\pi} \int_{-\pi}^{\pi} f_e^2(\theta_k) d\theta_k = 1$.

However, it is inconvenient to optimize θ_k and φ_k in a straightforward manner, since they are dependent variables and the dependence is difficult to capture for an arbitrary location of user k . Instead, we introduce orthogonal unit vectors $\vec{\mathbf{r}}_a \in \mathbb{R}^{3 \times 1}$ and $\vec{\mathbf{r}}_d \in \mathbb{R}^{3 \times 1}$, where $\|\vec{\mathbf{r}}_a\| = 1$, $\|\vec{\mathbf{r}}_d\| = 1$, and $\vec{\mathbf{r}}_a^T \cdot \vec{\mathbf{r}}_d = 0$, to denote the direction of the array axis and that of the dipole axis, respectively, cf. Fig. 2. We have

$$\cos \varphi_k = \vec{\mathbf{d}}_k^T \cdot \vec{\mathbf{r}}_a \quad (4)$$

$$\cos \theta_k = \vec{\mathbf{d}}_k^T \cdot \vec{\mathbf{r}}_d, \quad (5)$$

and $\vec{\mathbf{d}}_k = \vec{\mathbf{D}}_k / \|\vec{\mathbf{D}}_k\|$ is the unit direction vector of user k seen from the UAV.

B. Signal Model and Performance Metrics

Let $\mathbf{w}_k \in \mathbb{C}^{N \times 1}$ be the transmit beamforming vector for the low-priority user k , $k = 1, \dots, K$. The transmit signal of

the UAV is given as

$$\mathbf{s} = \sum_{k=1}^K \mathbf{w}_k \cdot s_k, \quad (6)$$

where $s_k \in \mathbb{C}$ is the data symbol intended for user k and $\mathbb{E}[|s_k|^2] = 1$, for all $k = 1, \dots, K$. As a result, the received signal of user k is given by

$$y_k = \mathbf{h}_k^H \sum_{k=1}^K \mathbf{w}_k \cdot s_k + n_k. \quad (7)$$

In (7), n_k denotes the effective noise plus interference (generated from e.g. the high-priority user and the environment) received at user k and is modeled as a Gaussian random variable with zero mean and variance σ_k^2 , for all $k = 1, \dots, K$. The achievable rate of user k in bps/Hz is

$$R_k = \log_2 \left(1 + \frac{|\mathbf{h}_k^H \mathbf{w}_k|^2}{\sum_{m=1, m \neq k}^K |\mathbf{h}_k^H \mathbf{w}_m|^2 + \sigma_k^2} \right). \quad (8)$$

Meanwhile, the interference power radiated towards the high-priority user is given by

$$P_1 = \sum_{k=1}^K |\mathbf{w}_k^H \mathbf{a}_{K+1}|^2, \quad (9)$$

where \mathbf{a}_{K+1} is the steering vector of the dipole array towards the high-priority user $K+1$, cf. (2).

Remark 1: In (9), \mathbf{a}_{K+1} and P_1 depend only on the direction of the high-priority user, θ_{K+1} and φ_{K+1} . That is, the user may locate at any point along $\vec{\mathbf{d}}_{K+1}$ and its exact position is unknown to the UAV. This differs from interference mitigation in cognitive radio and ground cellular networks which aims to suppress the *received* interference power of the users by assuming knowledge of the interference channel. But our problem formulation and solution proposed in Sections III and IV can also be easily extended to the latter case.

III. PROBLEM FORMULATION AND TRANSFORMATION

A. Problem Formulation

In (8) and (9), the beamforming vector \mathbf{w}_k and the antenna steering vector \mathbf{a}_k , the latter further depending on the orientation $\{\vec{\mathbf{r}}_a, \vec{\mathbf{r}}_d\}$ of the dipole array, are tightly coupled with each other to jointly determine the achievable rate R_k and radiated interference power P_1 . To exploit the benefits of the rotatable dipole array, we consider joint electrical beamforming and mechanical steering for maximization of the WSR of the low-priority users and minimization of interference power radiated toward the high-priority user. To this end, we assume that the positions of all low-priority users and the direction of the high-priority user are known to the UAV *a priori*. The resulting optimization problem is formulated as

$$\begin{aligned} \text{(P1) maximize} \quad & \sum_{k=1}^K \alpha_k \cdot R_k - \alpha_{K+1} \times P_1 \\ \text{subject to} \quad & \text{C1: } \|\mathbf{w}_k\|^2 \leq P_k, \quad k = 1, \dots, K \\ & \text{C2: } \|\vec{\mathbf{r}}_a\| = 1, \\ & \text{C3: } \|\vec{\mathbf{r}}_d\| = 1, \\ & \text{C4: } \vec{\mathbf{r}}_a^T \cdot \vec{\mathbf{r}}_d = 0. \end{aligned} \quad (10)$$

where α_k is the weight of achievable rate and radiated interference power with $\alpha_k \in [0, 1]$ and $\sum_{k=1}^{K+1} \alpha_k = 1$. In problem

(P1), constraint C1 limits the maximal transmit power allowable for low-priority user k by P_k , where $\sum_{k=1}^K P_k = P_{\max}$ and P_{\max} is the total transmit power of the UAV. In this paper, P_k is given a priori. But P_k can also be optimized using our problem formulation and solution. Constraints C2 and C3 enforce that $\vec{\mathbf{r}}_a$ and $\vec{\mathbf{r}}_d$ are unit direction vectors. Finally, C4 ensures that $\vec{\mathbf{r}}_a$ and $\vec{\mathbf{r}}_d$ are orthogonal to each other, due to the geometry of the considered ULA, cf. Fig. 2.

Problem (P1) is nonconvex as the objective function is non-concave and the constraints C2, C3 and C4 on array orientation are nonconvex. This type of problem is generally NP-hard, for which no efficient polynomial-time algorithms are known to optimally solve problem (P1) [9]. In the following, we will show that constraints C2, C3 and C4 have a special manifold structure, which can be exploited to facilitate real-time resource allocation via manifold optimization. Particularly, we will solve (P1) by proposing a low-complexity suboptimal algorithm which employs the proximal BCD and manifold optimization techniques to tackle the coupling between electrical beamforming and mechanical steering of the antenna array and the nonconvex constraints C2, C3 and C4, respectively.

B. Equivalent Problem Reformulation

Due to the nonconcave objective function, problem (P1) cannot be solved via proximal BCD and manifold optimization in a straightforward manner. This is because optimizing the beamforming vector \mathbf{w}_k for given antenna orientation $\{\vec{\mathbf{r}}_a, \vec{\mathbf{r}}_d\}$ would be a highly nonconvex optimization problem. Besides, optimizing $\{\vec{\mathbf{r}}_a, \vec{\mathbf{r}}_d\}$ for given \mathbf{w}_k would lead to an overly complicated manifold optimization problem.

Motivated by [15], we first reformulate (P1) as an *equivalent* weighted sum mean-square-error (MSE) and interference power minimization problem, so as to eliminate these obstacles. Let $u_k \in \mathbb{C}$ and $x_k \in \mathbb{R}$ be auxiliary optimization variables. The reformulated optimization problem is given by

$$\begin{aligned} \text{(P2) minimize} \quad & \sum_{k=1}^K \alpha_k (x_k e_k + \log_2 x_k) + \alpha_{K+1} P_1 \\ \text{subject to} \quad & \text{C1–C4}, \end{aligned} \quad (11)$$

where e_k is a function of u_k and \mathbf{w}_k given as

$$e_k = |u_k \mathbf{h}_k^H \mathbf{w}_k - 1|^2 + \sum_{m=1, m \neq k}^K |u_k \mathbf{h}_k^H \mathbf{w}_m|^2 + |u_k|^2 \sigma_k^2. \quad (12)$$

Problems (P2) and (P1) are equivalent in the sense that they have the same set of optimal solutions for beamforming \mathbf{w}_k and antenna orientation $\{\vec{\mathbf{r}}_a, \vec{\mathbf{r}}_d\}$ [15]. To verify this result, note that (P2) involves an unconstrained optimization over u_k and x_k . Based on the first-order optimality condition, the optimal solution of u_k and x_k can be derived in close form as,

$$u_k^* = \frac{\mathbf{h}_k^H \mathbf{w}_k}{\sum_{m=1}^K |\mathbf{h}_k^H \mathbf{w}_m|^2 + \sigma_k^2}, \quad (13)$$

$$x_k^* = e_k^{-1}. \quad (14)$$

The equivalence between problem (P2) and (P1) can be established by plugging (13) and (14) into (P2), whereby the latter reduces to the same objective function (except for a sign change) and constraints as (10).

Same as [15], u_k and e_k can be interpreted as the (single-antenna) receive beamformer of the low-priority user k and the

Algorithm 1 Proposed Proximal BCD Algorithm to Solve (P2)

Input: $\mathbf{W}_0 = [\mathbf{w}_{1,0}, \dots, \mathbf{w}_{K,0}]$, $\vec{\mathbf{r}}_{a,0}$, $\vec{\mathbf{r}}_{d,0}$ and $i = 1$

Output: Optimal $\mathbf{W} = [\mathbf{w}_1, \dots, \mathbf{w}_K]$, $\vec{\mathbf{r}}_a$ and $\vec{\mathbf{r}}_d$

- 1: **while** stopping criterion not met **do**
 - 2: Calculate $u_{k,i}^*$ and $x_{k,i}^*$ by (13) and (14) for $k = 1, \dots, K$.
 - 3: Solve (P3) for $\vec{\mathbf{r}}_d = \vec{\mathbf{r}}_{d,i-1}$ and $\vec{\mathbf{r}}_a = \vec{\mathbf{r}}_{a,i-1}$, and set $\mathbf{W}_i = \mathbf{W}$.
 - 4: Find an orthonormal basis ζ in the null space of $\vec{\mathbf{r}}_d = \vec{\mathbf{r}}_{d,i-1}$.
 - 5: Optimize γ_a in (P5) with RCG for $\mathbf{W} = \mathbf{W}_i$ and $\vec{\mathbf{r}}_d = \vec{\mathbf{r}}_{d,i-1}$.
 - 6: Calculate $\vec{\mathbf{r}}_a$ by (18) and set $\vec{\mathbf{r}}_{a,i} = \vec{\mathbf{r}}_a$.
 - 7: Optimize $\vec{\mathbf{r}}_d$ for $\mathbf{W} = \mathbf{W}_i$ and $\vec{\mathbf{r}}_a = \vec{\mathbf{r}}_{a,i}$, similar to Step 5, and set $\vec{\mathbf{r}}_{d,i} = \vec{\mathbf{r}}_d$.
 - 8: Update $i = i + 1$.
 - 9: **end while**
-

resulting MSE, respectively. Eq. (13) shows that the optimal solution of u_k is a minimum MSE (MMSE) receiver.

IV. PROBLEM SOLUTION

Problem (P2) is still nonconvex. To solve (P2), we present in this section the proposed iterative algorithm based on proximal BCD [16] and manifold optimization. The algorithm alternates between solving several subproblems of (P2), each for optimizing one of the five blocks of variables $\{u_k\}, \{x_k\}, \{\mathbf{w}_k\}, \{\vec{\mathbf{r}}_a\}, \{\vec{\mathbf{r}}_d\}$ while treating the other blocks of variables as fixed. To ensure that the obtained solution is also feasible to problems (P2) and (P1), we need to further tackle the coupling between $\{\vec{\mathbf{r}}_a\}$ and $\{\vec{\mathbf{r}}_d\}$ in constraint C4, cf. Sec. IV-B. Meanwhile, to ensure convergence of the algorithm, proximal terms are introduced into the objective function of problem (P2). We then discuss the solution for each subproblem, notably the ones involving manifold optimization.

A. Optimization of Beamforming

For convenience of presentation, let $f(u_k, x_k, \mathbf{w}_k, \vec{\mathbf{r}}_a, \vec{\mathbf{r}}_d)$ denote the objective function of problem (P2), where

$$f(u_k, x_k, \mathbf{w}_k, \vec{\mathbf{r}}_a, \vec{\mathbf{r}}_d) = \sum_{k=1}^K \alpha_k [x_k \cdot (|u_k \mathbf{h}_k^H \mathbf{w}_k - 1|^2 + \sum_{m \neq k} |u_k \mathbf{h}_k^H \mathbf{w}_m|^2)] + \alpha_{K+1} \sum_{k=1}^K |\mathbf{w}_k^H \mathbf{a}_{K+1}|^2. \quad (15)$$

Moreover, with a slight abuse of notation, $f(\mathbf{w}_k)$ and $f(\vec{\mathbf{r}}_a)$, or generally $f(\cdot)$, denote the objective function when the variables inside the parenthesis are to be optimized with the other variables of (P2) being fixed. Note that the optimal solutions of u_k and x_k for optimizing $f(u_k)$ and $f(x_k)$ are already given in (13) and (14), respectively. Further, the subproblem for optimizing the beamformer \mathbf{w}_k is defined as

$$(P3) \quad \underset{\mathbf{w}_k \in \mathbb{C}^{N \times 1}}{\text{minimize}} \quad f(\mathbf{w}_k) \quad (16) \\ \text{subject to} \quad \text{C1.}$$

(P3) is a convex optimization problem and can be tackled using off-the-shelf solvers such as CVX.

B. Optimization of Array Orientation

It remains to optimize the orientation of the antenna array $\{\vec{\mathbf{r}}_a, \vec{\mathbf{r}}_d\}$ with the other blocks of variables being fixed. In the following, we only show how to solve the subproblem of optimizing $\vec{\mathbf{r}}_a$. Exploiting the symmetry between $\vec{\mathbf{r}}_a$ and $\vec{\mathbf{r}}_d$, the subproblem of optimizing $\vec{\mathbf{r}}_d$ can then be tackled by simply interchanging $\vec{\mathbf{r}}_a$ and $\vec{\mathbf{r}}_d$ in the presented solution.

Let us define the following subproblem,

$$(P4) \quad \underset{\vec{\mathbf{r}}_a \in \mathbb{R}^{3 \times 1}}{\text{minimize}} \quad f(\vec{\mathbf{r}}_a) + c \cdot \|\vec{\mathbf{r}}_a - \vec{\mathbf{r}}_a'\|^2 \quad (17) \\ \text{subject to} \quad \text{C2, C4,}$$

where $c \geq 0$ and $\vec{\mathbf{r}}_a'$ records the solution of the direction vector $\vec{\mathbf{r}}_a$ in the last iteration. $c \cdot \|\vec{\mathbf{r}}_a - \vec{\mathbf{r}}_a'\|^2$ is a quadratic proximal term introduced to improve convergence of the iterations by convexifying problem (P4) and penalizing large deviations between the optimal solution of (P4) and $\vec{\mathbf{r}}_a'$.

Note that the feasible set of problem (P4) is a unit circle as it is the intersection of a unit sphere defined by constraint C2 and a plane defined by constraint C4. We now show that, thanks to this geometry structure, (P4) can be reformulated as a manifold optimization problem. To this end, let $\vec{\mathbf{r}}_d'$ be the direction of dipole axis obtained in the last iteration. Meanwhile, define $\zeta = [\zeta_1, \zeta_2] \in \mathbb{R}^{3 \times 2}$, where ζ_i , $i = 1, 2$ are the orthonormal bases for the null space of $\vec{\mathbf{r}}_d'$, and introduce $\gamma_a \in \mathbb{R}^{2 \times 1}$ as a new optimization variable with $\|\gamma_a\| = 1$. Finally, substituting $\vec{\mathbf{r}}_a$ in problem (P4) with γ_a according to

$$\vec{\mathbf{r}}_a = \zeta \cdot \gamma_a, \quad (18)$$

it can be reformulated as a standard manifold optimization problem given below,

$$(P5) \quad \underset{\gamma_a \in \mathbb{R}^{2 \times 1}}{\text{minimize}} \quad g(\gamma_a) \triangleq f(\zeta \cdot \gamma_a) + c \cdot \|\zeta \cdot \gamma_a - \vec{\mathbf{r}}_a'\|^2 \\ \text{subject to} \quad \text{C5: } \|\gamma_a\| = 1, \quad (19)$$

where constraint C5 defines a sphere manifold.

Problem (P5) can be solved using the Riemannian conjugate gradient descent (RCG) method, which is an extension of the conjugate gradient descent method (CG) on Riemannian manifolds. Let p be the iteration index of gradient descent and $\nabla_{\gamma_{a,p}} g$ be the Euclidean gradient of $g(\gamma_a)$ at $\gamma_a = \gamma_{a,p}$. The RCG method searches the next γ_a along direction $\boldsymbol{\eta}_p = -\text{grad}_{\gamma_{a,p}} g$, where $\text{grad}_{\gamma_{a,p}} g$ is the Riemannian gradient given by

$$\text{grad}_{\gamma_{a,p}} g = \nabla_{\gamma_{a,p}} g - \nabla_{\gamma_{a,p}} g \circ \gamma_{a,p} \circ \gamma_{a,p}. \quad (20)$$

Like the Euclidean gradient, the Riemannian gradient specifies the direction in which the objective function increases steepest in the Riemannian manifold space. Then, the next search point on the manifold is given by

$$\gamma_{a,p+1} = \text{unit}(\alpha_p \cdot \boldsymbol{\eta}_p), \quad (21)$$

where α_p is the search step size and can be chosen using e.g. the Armijo backtracking line search. In (21), $\text{unit}(\cdot)$ defines a retraction operation to keep the next search point on the manifold sphere, and hence feasible for problem (P5).

The RCG method is guaranteed to converge to a critical point of (P5), where the Riemannian gradient of the objective function vanishes [18]. Please also refer to [17] for more details about the RCG method. The overall algorithm for

solving (P2) is summarized in Algorithm 1. Note that the obtained solution is also feasible to problem (P1), and it can be further verified that it is a stationary point of (P1) [18].

V. SIMULATION RESULTS

In this section, we evaluate the performance of the proposed scheme via simulations. We consider a UAV equipped with a rotatable ULA. The UAV hovers at position $(6, 5, 20)$ for communicating with $K = 2$ low-priority users. We assume that the UAV has LoS channels to the users. The rotatable ULA comprises $N = 8$ half-wavelength dipole elements and neighboring dipole elements are separated by $d = \frac{\lambda}{2}$, where the carrier wavelength is $\lambda = 1$ mm. The maximal transmit power of the UAV is $P_{\max} = 10$ W and is equally shared by the low-priority users, i.e., $P_1 = P_2 = P_{\max}/2$, for fair resource allocation. Besides, we set all the weights in (P1) to $\alpha_k = 1/3$, $\forall k$. Finally, the noise power and the path loss coefficient are set as $\sigma_k^2 = 10^{-6}$ W, $\forall k$, and $\beta = 10^{-6}$ [4], respectively. For performance comparison, we consider the following schemes as benchmarks,

- *Baseline Scheme 1*: The UAV employs a rotatable ULA with isotropic elements.
- *Baseline Scheme 2*: The UAV employs a non-rotatable ULA with isotropic elements.

The orientation and/or the beamforming of Baseline Schemes 1 and 2 are optimized using Algorithm 1. For all considered schemes, the initial orientation of the directional antenna array in Algorithm 1 is set to $\vec{r}_{a,0} = (1, 0, 0)^T$ and/or $\vec{r}_{d,0} = (0, 0, 1)^T$.

Figure 3(a) shows the objective value of (P1) by employing Algorithm 1 with and without the proximal terms over 120 iteration steps, where the penalty factors in (P3)–(P5) are set to $c = 3$ and $c = 0$, respectively. Here, the low-priority users 1 and 2 are located at $(5, 5, 0)$ and $(10, 10, 0)$, respectively, while the position of the high-priority user 3 is $(6, 20, 15)$. From Figure 3(a) we observe that Algorithm 1 without proximal terms does not converge in the considered iteration steps. In contrast, Algorithm 1 with proximal terms quickly converges in a small number of iterations, thanks to the quadratic penalty function in the proximal term.

Figure 3(b) evaluates the gain in objective value of the Proposed Scheme and the Baseline Scheme 1 w.r.t. that of the Baseline Scheme 2, as the high-priority user 3 circles around the dipole axis with a radius of $\sqrt{6^2 + 20^2} \approx 20.9$ m and varying azimuth angles in the range $[0, \pi]$. Meanwhile, the low-priority users 1 and 2 are located at $(0, 7, 0)$ and $(6, 10, 0)$, respectively. From Figure 3(b) we observe that, compared with the Baseline Scheme 2, array rotation can almost double the optimal objective value when user 3 has the same azimuth angle w.r.t. the array axis as user 1 or 2. This results reveals that, even for an isotropic array, rotating the array orientation is beneficial as it can adjust the azimuth angles seen by different users in beamforming, cf. (2), to improve signal transmission and interference mitigation. Moreover, the proposed scheme can additionally exploit the directional antenna pattern of dipoles and the array rotation to achieve the best performance for all considered positions of the high-priority user. The Proposed Scheme achieves the maximal performance gains over the Baseline Scheme 1 when users 3 and 2 share the azimuth angle.

Figure 3(c) shows the sum-rate of the considered schemes for different number of antennas, when the low-priority users 1

and 2 are located at $(0, 7, 0)$ and $(6, 10, 0)$, respectively, while the position of the high-priority user 3 is $(6, 20, 15)$. By this setting, user 2, user 3, and the UAV are coplane with the initial direction of the dipole axis, $\vec{r}_{d,0} = (0, 0, 1)^T$, where the normal direction of the plane coincides with the initial direction of the array axis, $\vec{r}_{a,0} = (1, 0, 0)^T$. This would create a scenario of strong interference if the UAV starts transmission in the given array orientation. In particular, as the high-priority user 3 and the low-priority user 2 have the same azimuth angle w.r.t. the dipole ULA, the high-priority user 3 would be interfered by the beam towards the low-priority user 2. Figure 3(c) reveals that the performance gaps between the proposed and the baseline schemes enlarges as the number of antennas increases. Interestingly, the spatial DoFs provided by rotation and dipoles are most beneficial when exploited in systems with a small number of antennas. For example, the Baseline scheme 2 and the proposed scheme can improve the sum-rate (or objective value, since the interference power toward the high-priority user is negligible) by 180% and 300% when $N = 4$, respectively, compared to 106% and 265% when $N = 12$, respectively. This implies that the proposed scheme can be particularly advantageous for UAVs with limited SWAP.

For insights into the performance gains of rotatable dipole array, Figure 4 shows the optimized antenna array gain patterns, $|\mathbf{w}_k^H \mathbf{a}_k|^2$, of the considered schemes in the scenario of strong interference (cf. Figure 3(c)), where the dashed line denotes the communication direction of each user w.r.t. the UAV's antenna array. The gain patterns in Figure 4 are optimized using Algorithm 1. From Figure 4(a) we observe that the Baseline Scheme 2 mitigates the radiated interference to user 3 by simultaneously nulling the array gains in the direction towards user 2, which severely compromises the achievable rate of user 2. This is expected, since the Baseline Scheme 2 can only shape the array gain pattern via electrical beamforming. In contrast, Figure 4(b) shows that the Baseline Scheme 1 outperforms the Baseline Scheme 2 in balancing between interference mitigation and information broadcast. This is because, by using a rotatable ULA with isotropic elements, the Baseline Scheme 1 can steer the antenna array such that the low- and high-priority users can be separated in different azimuth angles. Consequently, the low-priority users can receive strong signal power without interfering the high-priority user. Finally, Figure 4(c) shows that, by using the rotatable dipole ULA, the proposed scheme can separate different users not only in different azimuth angles, but also in different elevation angles w.r.t. the antenna array. Consequently, the proposed scheme can shape gain patterns of different magnitudes for different users to best enhance information broadcast and, at the same time, suppress the radiated interference, which justifies the performance gains of the Proposed Scheme in Figure 3.

VI. CONCLUSIONS AND FUTURE WORK

In this paper, we considered joint electrical beamforming and mechanical steering using a rotatable dipole ULA for spectral-efficient interference-free UAV-aided multiuser downlink communication. To maximize the benefits of the rotatable dipole ULA, we formulated a nonconvex optimization problem for maximizing the WSR of low-priority users while minimizing the interference power radiated towards the high-priority user. Exploiting the problem structure, we further proposed an iterative algorithm based on proximal BCD and manifold

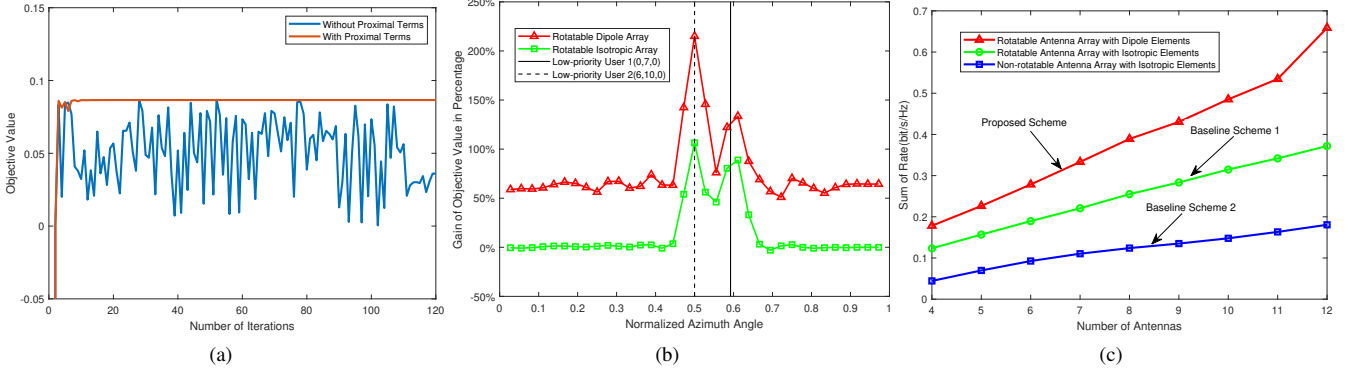


Fig. 3. (a) Convergence of Proposed Scheme and (b)–(c) performance comparison of considered schemes for (b) different positions of high-priority user and (c) different number of antennas.

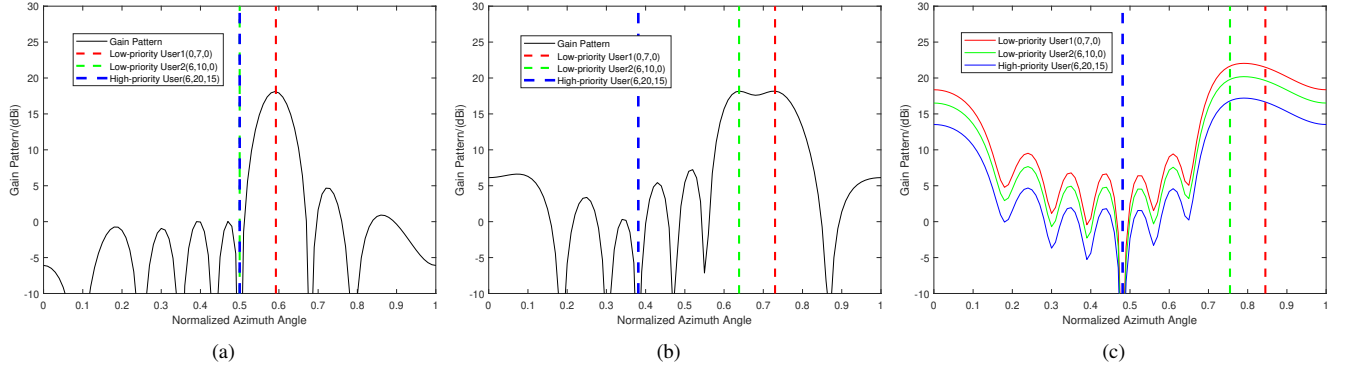


Fig. 4. Optimized array gain patterns of (a) Baseline Scheme 2, (b) Baseline Scheme 1, and (c) Proposed Scheme.

optimization to solve the nonconvex optimization problem. Our simulation results verified the convergence of the proposed algorithm and showed that the rotatable dipole ULA achieves both higher sum-rate (e.g. claiming up to 300% gains) and lower radiated interference than the rotatable and non-rotatable ULAs with isotropic antenna elements. This is because through joint electrical beamforming and mechanical steering, the rotatable dipole ULA can not only separate the low- and high-priority users in different azimuth angles, but also optimize the gain patterns for users in different elevation angles. In contrast, interference could be non-avoidable by beamforming using a non-rotatable array with isotropic elements when the low- and high-priority users see the same azimuth angle from the UAV. In this paper, as we focus on investigating the 3D rotation of dipole antenna array, we have assumed that the UAV keeps hovering at given position. Joint optimization of rotation, translation (via trajectory planning), and beamforming for dipole array or other types of arrays/apertures of directional antennas (such as patch antennas) are left as interesting topics for future consideration.

REFERENCES

- [1] W. Chen, X. Lin, J. Lee, et al., “5G-advanced towards 6G: Past, present, and future”, *IEEE J. Sel. Area Commun.* (accepted), 2023.
- [2] Q. Wu, J. Xu, Y. Zeng, et al., “A comprehensive overview on 5G-and-beyond networks with UAVs”, *IEEE J. Sel. Areas Commun.*, vol. 39, no. 10, pp. 2912-2945, Oct. 2021.
- [3] J. Wang, X. Wang, R. Gao et al., “Physical layer security for UAV Communications in 5G and beyond networks,” arXiv:2015.11332, 2021. [Online]. Available: <https://arxiv.org/abs/2105.11332>.
- [4] Z. Lyu, G. Zhu and J. Xu, “Joint maneuver and beamforming design for UAV-enabled integrated sensing and communication,” *IEEE Trans. Wireless Commun.*, vol. 22, no. 4, pp. 2424-2440, April 2023.
- [5] C. Deng, X. Fang and X. Wang, “Beamforming design and trajectory optimization for UAV-empowered adaptable integrated sensing and communication,” *IEEE Trans. Wireless Commun.* (accepted), Apr. 2023.
- [6] S. Zhang, Y. Zeng and R. Zhang, “Cellular-enabled UAV communication: A connectivity-constrained trajectory optimization perspective,” *IEEE Trans. Commun.*, vol. 67, no. 3, pp. 2580-2604, Mar. 2019.
- [7] Z. Xiao, L. Zhu, Y. Liu, et al., “A survey on millimeter-wave beamforming enabled UAV communications and networking,” *IEEE Commun. Surveys Tuts.*, vol. 24, no. 1, pp. 557-610, First Quarter, 2022.
- [8] L. Liu, S. Zhang and R. Zhang, “Multi-beam UAV communication in cellular uplink: Cooperative interference cancellation and sum-rate maximization,” *IEEE J. Sel. Areas Commun.*, vol. 35, no. 10, pp. 2370-2382, Jul. 2019.
- [9] L. Xiang, L. Lei, S. Chatzinotas, et al., “Towards power-efficient aerial communications via dynamic multi-UAV cooperation,” in *Proc. IEEE WCNC*, 2020, pp. 1–7.
- [10] J. Zhang, H. Xu, L. Xiang et al., “On the application of directional antennas in multi-tier unmanned aerial vehicle networks,” *IEEE Access*, vol. 7, pp. 132095-132110, 2019.
- [11] G. Lu, J. Zhang, L. Xiang et al., “A global optimization method for energy-minimal UAV-aided data collection over fixed flight path,” in *Proc. IEEE ICC*, May 2022.
- [12] E. Owolola, K. Xia, T. Wang, et al., “Pattern synthesis of uniform and sparse linear antenna array using Mayfly algorithm,” *IEEE Access*, vol. 9, pp. 77954-77975, May 2021.
- [13] Y. Zeng, R. Zhang, and T. J. Lim, “Wireless communications with unmanned aerial vehicles: Opportunities and challenges,” *IEEE Commun. Mag.*, vol. 54, no. 5, pp. 36-42, May 2016.
- [14] C. A. Balanis, *Antenna Theory: Analysis and Design*. John Wiley & Sons, 4th edition, 2016.
- [15] Q. Shi, M. Razaviyayn, Z. Luo et al., “An Iteratively Weighted MMSE Approach to Distributed Sum-Utility Maximization for a MIMO Interfering Broadcast Channel,” *IEEE Trans. Signal Process.*, vol. 59, no. 9, pp. 4331-4340, Sep. 2011.
- [16] J. Bolte, S. Sabach and M. Teboulle, “Proximal alternating linearized minimization for nonconvex and nonsmooth problems,” *Mathematical Programming*, vol. 146, no. 1-2, pp. 459-494, Oct. 2014.
- [17] X. Yu, D. Xu, and R. Schober, “MISO Wireless Communication System via Intelligent Reflecting Surfaces,” in *Proc. IEEE/CIC ICC*, Aug. 2019.
- [18] P.-A. Absil, R. Mahony and R. Sepulchre, *Optimization Algorithms on Matrix Manifolds*. Princeton University Press, 2009.